

to 3 mL again; this was repeated three times and the mixture was finally evaporated to dryness. The residue was dissolved in 100 mL of warm methanol, silica gel (2 g) was added to the methanolic solution, and the solution was evaporated to dryness. The residue was loaded onto a column of silica gel and was eluted with CHCl_3 -MeOH (9:1). Pooled fractions on evaporation gave 10 as a colorless solid (100 mg, 39%): R_f 0.1 (CHCl_3 -MeOH, 9:1); mp 244-245 °C; UV λ_{max} (nm) 270 (CH_3OH , ϵ 12900), 264 (0.1 N HCl), 274 (pH 7 buffer), 276 (0.1 N NaOH); ^1H NMR ($(\text{CD}_3)_2\text{SO}$) δ 2.93-2.96 (m, 1, 5'-H), 3.41-3.45 (m, 1, 5'-H), 3.94 (d, 1, 4'-H), 4.20 (d, 1, 3'-H), 4.35 (m, 1, 2'-H), 5.1-5.4 (br s, 2, OH's), 5.81 (s, 1, 1'-H), 6.33-6.34 (m, 1, NH), 6.86 and 6.99 (br s, 2, NH_2), 7.42 (s, 1, C2-H); ^{13}C NMR ($(\text{CD}_3)_2\text{SO}$) δ 49.37 (t, C-5'), 71.52 (d, C-4'), 76.99 (s, C-3'), 87.69 (d, C-2'), 92.42 (d, C-1'), 115.72 (br s, CONH_2), 128.97 (d, C-2), 143.80 (s, C-5), 166.38 (s, C-4); mass spectrum, m/e 240 ($\text{C}_6\text{H}_{12}\text{N}_4\text{O}_4^+$).

Anal. Calcd for $\text{C}_9\text{H}_{12}\text{N}_4\text{O}_4 \cdot 0.5\text{H}_2\text{O}$: C, 43.37; H, 5.26; N, 22.48. Found: C, 43.57; H, 4.97; N, 22.13.

Conditions Used for the HPLC Separation of Nucleosides, Cyclonucleosides, and Their Hydrolysis Products. HPLC was carried out on an IBM LC/9533 system using an IBM C-18 reversed phase column and a 20- μL injection loop. Elution was carried out with continuous UV detection of the eluant at 254 nm as follows. Solvent A (5% methanol in 0.1 M ammonium dihydrogen phosphate solution (no adjustment to pH made), flow rate 2.0 mL/min) gives adenine (5.2 min), adenosine (13.9 min), cycloadenosine (4.8 min) and its hydrolysis product (14.6 min), guanine (3.1 min), guanosine (5.1 min), cycloguanosine (5.3 min) and its hydrolysis product (2.6 min), 7-methylguanosine (2.1 min), 7-methylguanine (6.2 min), and 7-methylcycloguanosine (3.3 min) and its hydrolysis product (7.4 min). Solvent B (1% methanol in 0.1 M ammonium dihydrogen phosphate solution, flow rate 0.5 mL/min) gives cycloadenosine salt (10.7 min) and its hydrolysis product (11.7 min) and guanine (16.0 min). Solvent C (1% methanol in 0.1 M ammonium dihydrogen phosphate solution, flow rate 2.0 mL/min) gives AICAR (13.3 min) and AICA (4.8 min).

Product Characterization of Glycosidic Hydrolysis Reactions. For preparative scale reactions using the cyclonucleosides, the hydrolyses were repeated at higher concentrations and allowed to proceed for at least 6 half-lives, after which the homogeneity of the product was determined by HPLC. UV absorption spectra of each product solution was taken at acidic, neutral, and basic pH's and compared to spectra of analogous purine standards as described. Finally, each reaction mixture was lyophilized to provide solid samples that were characterized by fast atom bombardment mass spectrometry. Unless specifically

mentioned, every hydrolysis product appeared as a single peak on HPLC.

Glycosidic hydrolysis product from 5',8-cycloadenosine (2): UV λ_{max} (nm) 268 (0.1 N HCl), 266 (pH 7 buffer), 272 (0.1 N NaOH) [compare to adenine 263 (0.1 N HCl), 261 (pH 7 buffer), 269 (0.1 N NaOH)]; FAB mass spectrum, m/e 268 ($\text{C}_{10}\text{H}_{14}\text{N}_5\text{O}_4^+$).

Glycosidic hydrolysis product from 5',8-cycloguanosine (4): UV λ_{max} (nm) 254 (0.1 N HCl), 236 (pH 7 buffer), 276 (0.1 N NaOH) [compare to guanine 250 (0.1 N HCl), 244 (pH 7 buffer), 269 (0.1 N NaOH)]; FAB mass spectrum, m/e 284 ($\text{C}_{10}\text{H}_{14}\text{N}_5\text{O}_5^+$).

Glycosidic Hydrolysis Product from 3,5'-Cycloadenosine Salt 6. This reaction product has previously been prepared and characterized.²⁰ Our reaction product proved identical with that reported.

Glycosidic hydrolysis product from 7-methyl-5',8-cycloguanosine (8): UV λ_{max} (nm) 256 (0.1 N HCl), 250 (pH 7 buffer), 282 (0.1 N NaOH) [compare to 7-methylguanine 252 (0.1 N HCl), 250 (pH 7 buffer), 282 (0.1 N NaOH)]; FAB mass spectrum, m/e 298 ($\text{C}_{11}\text{H}_{16}\text{N}_5\text{O}_5^+$). To insure that the purine ring system was not undergoing acid-catalyzed hydration (as is known to occur under basic conditions), we heated a sample of 7,9-dimethylguanine⁴⁶ at 90 °C in 0.1 N HCl for 24 h; during this time, no change was observed in the solution's HPLC trace, which was identical with that obtained by using a solution of 7,9-dimethylguanine itself.

Glycosidic Hydrolysis Product from Cyclo-AICAR Derivative 10. HPLC of this reaction performed in 0.1 N HCl does not reveal the clean conversion of starting material and concurrent formation of a single product seen in all other reactions, but rather demonstrated the production of at least three reaction products all forming on about the same time frame.

Glycosidic Hydrolysis Product from 5'-Amino-5'-deoxyadenosine. The UV absorbing product of glycosidic cleavage, namely adenine, eluted identically with that of authentic adenine in several solvent systems.

Acknowledgment. The variously timed financial support of the American Cancer Society and the American Heart Association (Central Ohio Chapter) are acknowledged with gratitude. We thank Merck and Company for making a postdoctoral fellowship available that greatly facilitated this research. X.M.C. thanks the Government of India for providing a National Fellowship. Lastly, we appreciate the constructive comments made by two reviewers that substantially improved the quality of this manuscript.

Skeletal Deformation in 4,5-Disubstituted 9,10-Dihydrophenanthrenes and 4,5-Disubstituted Phenanthrenes

Robert Cosmo, Trevor W. Hambley, and Sever Sternhell*

Department of Organic Chemistry, University of Sydney, New South Wales 2006, Australia

Received February 20, 1987

Single-crystal X-ray structures were determined for six 9,10-dihydro-4,5-di-X-phenanthrenes (1, X = H, F, OMe, Cl, Me, CF_3) and four 4,5-di-X-phenanthrenes (2, X = F, Cl, Me, CF_3). Skeletal deformation in both series appears to be simply related to the apparent overlap between the X groups.

We have previously proposed a simple measure of steric stress (apparent overlap, Σr^*)¹ and shown that it correlates well with the energy required to overcome the stress in rotation in biphenyls,¹ meso-tetraarylporphyrins,² 9,10-

dihydrophenanthrenes,³ and N-arylsuccinimides.⁴

Examination of models reveals that intramolecular distances between substituents at C-4 and C-5 in both phenanthrenes and dihydrophenanthrenes are shorter than the sums of their van der Waals radii, even for the case of hydrogen⁵ and this was expected to cause distortions

(1) Bott, G.; Field, L. D.; Sternhell, S. *J. Am. Chem. Soc.* 1980, 102, 5618.

(2) Crossley, M. J.; Field, L. D.; Forster, A. J.; Harding, M. M.; Sternhell, S. *J. Am. Chem. Soc.* 1987, 109, 341.

(3) Cosmo, R.; Sternhell, S. *Aust. J. Chem.* 1987, 40, 35.

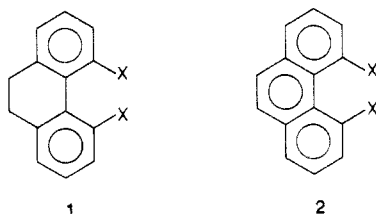
(4) Newsom, I. A. Ph.D. Thesis, University of Sydney, 1983.

Table I. Selected Structural Parameters of 4,5-Disubstituted 9,10-Dihydrophenanthrenes

X	$\Sigma\theta$, deg	$\Sigma d $, Å	α , deg	β , deg	$d_{4,5}$, Å	ϕ_{AB} , deg	$\phi_{BB'}$, deg	$\phi_{AA'}$, deg	γ_{X-4-3} , deg	γ_{X-4-4a} , deg	Σr^* , Å
H	5.1	0.007	21.2	20.2	3.004	57	64	177	118	120	0.45
F	20.1	0.117	36.1	29.7	3.153	60	60	180	117	119	1.18
OCH ₃	27.1	0.149	42.0	32.8	3.165	55	69	179	123	117	1.31
Cl	33.7	0.198	47.4	35.3	3.237	63	56	178	117	121	1.96
CH ₃	31.6	0.187	45.6	36.6	3.212	62	57	179	118	124	2.21
CF ₃	35.5	0.216	46.7	39.0	3.324	56	58	170	114	124	3.04

within the molecular frameworks. The purpose of this study was to explore the relationship between the steric stress as defined by apparent overlap¹ and steric strain manifesting itself as skeletal distortion in the title series.

Within a series of 4,5-disubstituted 9,10-dihydrophenanthrenes (1) or 4,5-disubstituted phenanthrenes (2),



the parameters relating to the distortion of the C-X bond are not necessarily expected to correlate well with the size of the X group, because of the differing characteristics of various C-X bonds. For the same reason, the pyramidalization parameter⁶ for C-4 (C-5) was considered less significant than structural parameters relating to deformation remote from C-4 and C-5.

4,5-Disubstituted 9,10-Dihydrophenanthrenes. In the series of 4,5-disubstituted 9,10-dihydrophenanthrenes (1) the structural parameters (Figure 1) that may be of interest as measures of strain include the following. (1) The sum of the absolute values of the torsion angles, $\Sigma\theta$, defined by carbons in the benzene rings. The torsion angle θ of carbons A, B, C, and D is defined as the angle between the plane defined by carbons A, B and C and the plane defined by carbons B, C, and D. (2) The sum of the distortions, $\Sigma|d|$, of the carbons from the least-squares plane of the benzene rings. (3) The dihedral angles between the benzene rings. These can be defined either in terms of the torsion angle (α) of C-4, C-4a, C-5a, C-5 or the torsion angle (β) of C-10a, C-4a, C-5a, C-9a. (4) The distance between C-4 and C-5 ($d_{4,5}$). (5) The dihedral angles between the methylene protons (ϕ_{AB} , $\phi_{BB'}$, $\phi_{AA'}$). (6) The angles between the X group and C-3, C-4, C-4a denoted as γ_{X-4-3} and γ_{X-4-4a} .

These parameters, illustrated diagrammatically in Figure 1, are summarized for all the dihydrophenanthrenes in Table I, the data being derived from the atomic coordinates in the supplementary material.

As expected the parameters relating to the deformation of the C-X bond, γ_{X-3-4} and γ_{X-4-4a} , do not show any correlation with the size of the X substituent and the dihedral angles, ϕ , are essentially invariant for all the 9,10-dihydrophenanthrenes. Thus the ground-state conformation of the methylene protons is essentially the same over a wide range of substituents at C-4 and C-5. This conclusion was also independently drawn from the analyses of the ¹H NMR. AA'/BB' spin systems,³ where the coupling constants were found to be essentially constant for all compounds analyzed. The most pronounced difference in

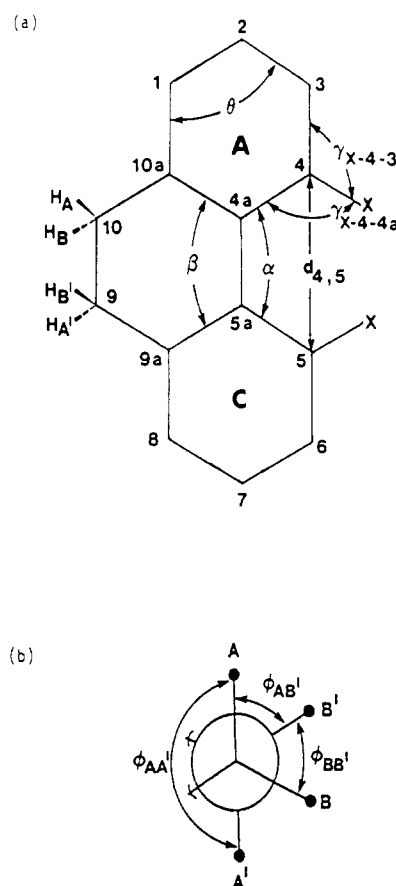


Figure 1. (a) Systematic numbering of the 9,10-dihydrophenanthrene nucleus and the definition of certain structural parameters of interest. (b) Dihedral angles between the methylene protons of 9,10-dihydrophenanthrenes.

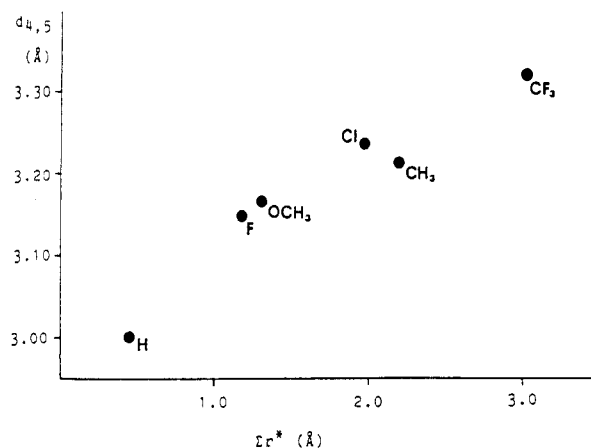


Figure 2. Plot of $d_{4,5}$ against the apparent overlap, Σr^* , in 4,5-disubstituted 9,10-dihydrophenanthrenes.

the dihedral angles of the methylene protons is the trans diaxial dihedral angle, $\phi_{AA'}$, of 9,10-dihydro-4,5-bis(trifluoromethyl)phenanthrene, 170°, compared with values of 177–180° obtained for the other 9,10-dihydrophenanthrenes. This is consistent with the analyses of the

(5) Kay, M. I.; Okaya, Y.; Cox, D. E. *Acta Crystallogr. Sect. B* 1971, B27, 26.

(6) Dunitz, J. D. *X-ray Analysis and the Structure of Organic Molecules*; Cornell University Press: Ithaca, NY, 1979; Chapter 7, pp 328–337.

Table II. Selected Structural Parameters of 4,5-Disubstituted Phenanthrenes

X	$\Sigma\theta$, deg	$\Sigma d $, Å	α , deg	β , deg	$d_{4,5}$, Å	γ_{X-4-3} , deg	γ_{X-4-4a} , deg	Σr^* , Å
H ^a	3.7	0.017	2.6	1.5	2.997	119	121	0.60
F	27.0	0.157	20.1	12.7	3.150	116	120	1.38
Cl	42.2	0.254	37.7	24.1	3.211	116	122	2.28
CH ₃	43.2	0.252	33.0	22.2	3.155	118	124	2.62
CF ₃	49.3	0.298	34.0	25.4	3.271	113	125	3.50

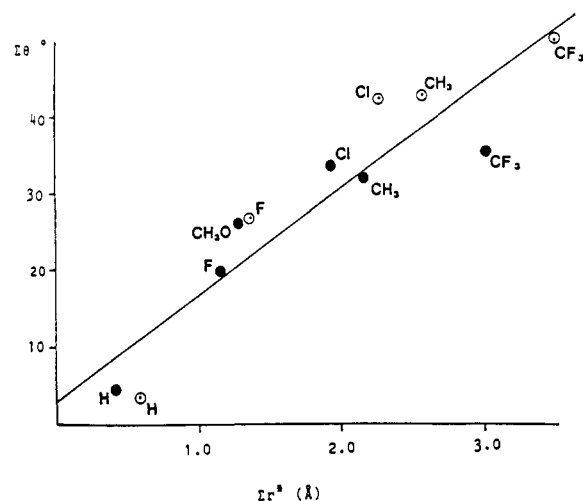
^a Data from ref 5.

Figure 3. Plot of $\Sigma\theta$ against apparent overlap, Σr^* , in 4,5-disubstituted 9,10-dihydrophenanthrenes (●) and 4,5-disubstituted phenanthrenes (○). (Line of best fit, $R = 0.92$; $\Sigma\theta = 3.0 + 13.9\Sigma r^*$).

AA'BB' spin system of this compound in two solvents in which $J_{AA'}$ was found to be smaller³ than in the other 9,10-dihydrophenanthrenes.

The other parameters listed in Table I show a much more obvious trend with apparent overlap¹ (Σr^*).

The plots of $d_{4,5}$ and $\Sigma\theta$ against the apparent overlap in the 9,10-dihydrophenanthrene are shown in Figures 2 and 3. The plots indicate a reasonable monotonicity between these distortions of the molecular framework of 9,10-dihydrophenanthrenes and the stress associated with the nonbonded interactions of the 4,5-substituents, as expressed by the apparent overlap parameter, Σr^* .

4,5-Disubstituted Phenanthrenes. In a series of 4,5-disubstituted phenanthrenes (2) the parameters of interest include the following: (1) The sum of the torsion angles, $\Sigma\theta$, of the carbons in rings A and C. (2) The sum of the distortions, $\Sigma|d|$, of the carbons from the average plane of the A and C rings. (3) The dihedral angles between the A and C rings. These can be defined either in terms of the torsion angle (α) of C-4, C-4a, C-5a, C-5 or the torsion angle (β) of C-10a, C-4a, C-5a, C-9a. (4) The distance between C-4 and C-5 ($d_{4,5}$). (5) The angles between the X group and C-3, C-4, C-4a denoted as γ_{X-4-3} and γ_{X-4-4a} .

These parameters for the 4,5-disubstituted phenanthrenes are defined in Figure 4 and listed in Table II.

Phenanthrene is an often-quoted example⁵ of molecular deformation due to nonbonded interactions. However, the distortions in phenanthrene are comparable to those in 9,10-dihydrophenanthrene and are almost negligible compared to those in 4,5-disubstituted derivatives determined in this work (Table II).

Once again, as expected, there is no monotonic trend in the parameters, γ , relating to the distortion of the C-X bond.

The plots of $d_{4,5}$ and $\Sigma\theta$ against the apparent overlap in the 4,5-disubstituted phenanthrenes are shown in Figures 5 and 3, respectively.

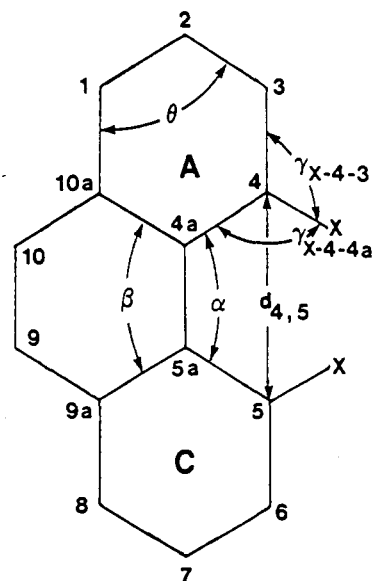


Figure 4. Systematic numbering of the phenanthrene nucleus and the definition of certain structural parameters of interest.

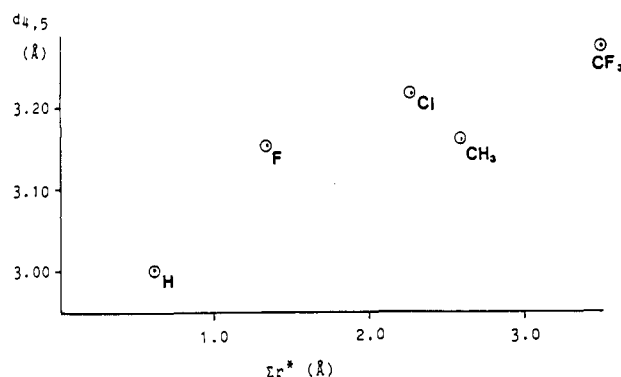


Figure 5. Plot of $d_{4,5}$ against apparent overlap, Σr^* , in 4,5-disubstituted phenanthrenes.

The plots indicate an essentially monotonic relationship between the distortions of the molecular framework of 4,5-disubstituted phenanthrenes and the stress associated with the nonbonded interactions of the 4,5-substituents, as expressed by the apparent overlap parameter, Σr^* .

The most obvious deviation from the monotonic relationships is the relative position of the data for chlorine and methyl (Figures 2, 3, and 5). This may be due to the fact that the methyl-methyl interactions may be lessened by cog-wheeling⁷ but the measurement of apparent overlap assumes the methyl group to be a sphere of 1.8 Å in radius,¹ thus overestimating slightly its effective size. The relationships summarized in Tables I and II and Figures 2, 3, and 5 suggest that the apparent overlap parameter could be used to predict, at least semiquantitatively, the distortions from ideal bond lengths and angles in crowded molecules.

Table III. Crystal Data for the 9,10-Dihydrophenanthrenes^a

	1, X = H	1, X = F	1, X = OCH ₃	1, X = Cl	1, X = CH ₃	1, X = CF ₃
crystal system	orthorhombic	monoclinic	monoclinic	monoclinic	triclinic	orthorhombic
space group	<i>P</i> 2 ₁ 2 ₁ 2 ₁	<i>P</i> 2 ₁ / <i>c</i>	<i>Cc</i>	<i>C</i> 2/ <i>c</i>	<i>P</i> 1	<i>F</i> 2 <i>dd</i>
cell constants						
<i>a</i> , Å	7.933 (3)	8.068 (2)	9.363 (1)	9.478 (2)	7.242 (2)	8.828 (3)
<i>b</i> , Å	16.746 (3)	11.983 (2)	12.423 (1)	13.455 (2)	8.053 (1)	13.489 (3)
<i>c</i> , Å	30.20 (1)	10.526 (1)	12.007 (2)	9.377 (2)	10.535 (2)	22.480 (4)
α , deg					80.72 (1)	
β , deg		92.01 (2)	112.99 (1)	104.78 (2)	78.78 (1)	
γ , deg					79.62 (1)	
<i>V</i> , Å ³	4011.7	1017.1	1285.6	1156.3	587.7	2676.9
<i>D</i> _{calc} , g cm ⁻³	1.193	1.412	1.241	1.689	1.177	1.569
mol form	C ₁₄ H ₁₂	C ₁₄ H ₁₀ F ₂	C ₁₆ H ₁₆ O ₂	C ₁₄ H ₁₀ Cl ₂	C ₁₆ H ₁₆	C ₁₆ H ₁₀ F ₆
mol wt	180.2	216.2	240.3	294.1	208.3	316.2
<i>Z</i>	16	4	4	4	2	8
<i>F</i> (000), electrons	1536	448	512	512	224	1280
absn coeff, cm ⁻¹	0.34	0.65	0.45	4.69	0.33	1.02
cryst degrad	10%	<2%	<2%	<2%	<2%	<2%
temp, K	128	128	294	294	294	294
scan mode	ω -1.67 θ	ω - θ	ω -1.67 θ	ω - θ	ω -1.67 θ	ω - θ
2 θ range, deg	1.0-50.0	1.0-50.0	1.0-50.0	1.0-50.0	1.0-50.0	1.0-50.0
<i>hkl</i> measured	$+h, +k, +l$	$\pm h, +k, +l$	$+h, +k, \pm l$	$+h, +k, \pm l$	$+h, \pm k, \pm l$	$+h, +k, +l$
reflcns measd	4727	2283	1311	1536	2391	713
merging <i>R</i>		0.03	0.01	0.01	0.01	0.01
reflcns used	3552	1557	865	744	1518	580
<i>I</i> > 2.5 σ (<i>I</i>)						
no. of variables	698	186	170	94	210	120
<i>R</i>	0.048	0.048	0.027	0.032	0.033	0.029
<i>R</i> _w	0.051	0.049	0.031	0.037	0.041	0.031
$w[=g/(\sigma^2 F_o + kF_o^2)]$, <i>g</i> , <i>k</i>	4.55, 0.00038	1.00, 0.0035	2.11, 0.00023	1.00, 0.0012	1.00, 0.00096	1.54, 0.00009
shift/esd	<0.2	<0.3	<0.1	<0.01	<0.01	<0.2
resid extrema in final diff map, e Å ⁻³	±0.25	±0.35	±0.20	±0.20	±0.14	±0.15

^a Diffractometer, Enraf-Nonius CAD4-F; radiation, Mo K α (λ 0.71069 Å); monochromator, graphite.Table IV. Crystal Data for the Phenanthrenes^a

	2, X = F	2, X = Cl	2, X = CH ₃	2, X = CF ₃
crystal system	monoclinic	orthorhombic	monoclinic	orthorhombic
space group	<i>C</i> 2/ <i>c</i>	<i>P</i> <i>b</i> <i>cn</i>	<i>P</i> 2 ₁	<i>F</i> 2 <i>dd</i>
cell constants				
<i>a</i> , Å	10.531 (1)	13.009 (3)	8.318 (1)	9.108 (1)
<i>b</i> , Å	10.789 (2)	11.901 (2)	8.281 (1)	13.454 (2)
<i>c</i> , Å	17.703 (4)	7.071 (2)	8.746 (2)	20.756 (4)
β , deg	104.73 (1)		107.62 (1)	
<i>V</i> , Å ³	1946.9	1094.8	574.2	2543.4
<i>D</i> _{calc} , g cm ⁻³	1.461	1.499	1.193	1.641
mol form	C ₁₄ H ₈ F ₂	C ₁₄ H ₈ Cl ₂	C ₁₆ H ₁₄	C ₁₆ H ₈ F ₆
mol wt	214.2	247.1	206.3	314.2
<i>Z</i>	8	4	2	8
<i>F</i> (000), electrons	880	504	220	1264
absn coeff, cm ⁻¹	0.68	4.96	0.34	1.08
cryst degrad	<2%	<2%	<2%	<2%
temp, K	294	294	294	294
scan mode	ω -0.33 θ	ω -0.67 θ	ω -0.67 θ	ω - θ
2 θ range, deg	1.0-50.0	1.0-50.0	1.0-50.0	1.0-50.0
<i>hkl</i> measd	$\pm h, +k, +l$	$+h, +k, +l$	$+h, +k, \pm l$	$+h, +k, +l$
reflcns measd	1941	1219	1240	1293
merging <i>R</i>	0.01		0.01	
reflcns used	1111	717	893	591
<i>I</i> > 2.5 σ (<i>I</i>)				
no. of variables	178	90	201	116
<i>R</i>	0.038	0.029	0.037	0.024
<i>R</i> _w	0.043	0.035	0.042	0.029
$w[=g/(\sigma^2 F_o + kF_o^2)]$, <i>g</i> , <i>k</i>	1.26, 0.00040	1.12, 0.00030	1.76, 0.00015	2.47, 0.00011
shift/esd	<0.1	<0.1	<0.3	<0.1
resid extrema in final diff map, e Å ⁻³	±0.20	±0.20	±0.10	±0.15

^a Diffractometer, Enraf-Nonius CAD4-F; radiation, Mo K α (λ 0.71069 Å); monochromator, graphite.

Somewhat surprisingly, it also appears that the degree of distortion of the benzene rings of 9,10-dihydro-4,5-di-X-phenanthrenes and the corresponding skeletal distortions in 4,5-di-X-phenanthrenes bears *similar* relationships to the apparent overlap between the 4,5-substituents. This is illustrated by the plot of $\Sigma\theta$ (Figure 3) against the apparent overlap for both series of compounds. Thus at least

in some ways, both series are "similarly distortable".

The strain manifests itself in all structures in a similar way. The rings labeled A and C in both 9,10-dihydrophenanthrenes (Figure 1) and phenanthrenes (Figure 4) are folded about the C-2,C-4a axis with C-4a more out of plane. These two rings also rotate with respect to one another about the C-4a,C-5a bond.

Clearly, the skeletal distortions correlated above with apparent overlap would show simple relationships with parameters that are either inherently related to the apparent overlap parameter, such as van der Waals radii or Charton's effective steric parameters,⁸ or that were shown to be related to apparent overlap, such as the inversion barriers in 4,5-disubstituted 9,10-dihydrophenanthrenes.³

Experimental Section

Materials. The preparation of the ten compounds used for crystallographic work is described elsewhere.^{3,9}

Crystallographic Data. Crystals were mounted on glass fibers by using cyanoacrylate resin. Data were collected on an Enraf-Nonius CAD4-F diffractometer with Mo K α radiation. Unit cell dimensions were determined by a least-squares fit to the setting angles of 25 independent reflections in the range $15 < 2\theta < 25^\circ$. Crystal data are collected in Tables III and IV.

The structures were solved by direct methods using SHELX-76¹⁰ and refined by full-matrix least-squares methods. All hydrogen atoms were refined with isotropic temperature factors and non-hydrogen atoms were refined anisotropically. Scattering factors used were those provided in SHELX-76. Tables of structure factors, bond lengths and angles, and atom positional and thermal parameters have been deposited as supplementary material.

Calculation of apparent overlap (Σr^*) follows the procedure described earlier¹ and is fully detailed in the supplementary material.

Supplementary Material Available: Tables of X-ray crystallographic data and ORTEP drawings for a series of 4,5-disubstituted 9,10-dihydrophenanthrenes and 4,5-disubstituted phenanthrenes and procedures for calculation of apparent overlap (Σr^*) (39 pages); tables of observed and calculated structure factors for the 4,5-disubstituted 9,10-dihydrophenanthrenes and 4,5-disubstituted phenanthrenes (71 pages). Ordering information is given on any current masthead page.

(8) Charton, M. *Top. Curr. Chem.* 1983, 114, 57.

(9) Cosmo, R. Ph.D. Thesis, University of Sydney, 1986.

(10) Sheldrick, G. M. SHELX-76, A Program for X-ray Crystal Structure Determination, University of Cambridge, 1976.

Supercritical Carbon Dioxide.^{1,2} The Cis to Trans Relaxation and π, π^* Transition of 4-(Diethylamino)-4'-nitroazobenzene

Michael E. Sigman and John E. Leffler*

Department of Chemistry, Florida State University, Tallahassee, Florida 32306

Received February 9, 1987

Rates of the cis-trans isomerization of 4-(diethylamino)-4'-nitroazobenzene (DENAB) have been determined for supercritical CO₂ media at 32.4 °C and several densities and DENAB concentrations. A plot of ΔG^\ddagger against the Kamlet-Taft π^* solvent parameter has two linear parts, one for the CO₂ media and alkanes and another for more polar solvents. The slope for the CO₂ and alkanes is positive and small, and that for the other solvents is large and negative. It is suggested that the reaction mechanism in the CO₂ media and in alkanes is inversion at one of the azo nitrogens, while in the more polar solvents it is rotation about the bond between the azo nitrogens, for which the transition state is much more polar. The point of intersection of the two lines is at a π^* value of about +0.2. Unlike the ΔG^\ddagger values, the E_{max} of the π, π^* internal charge-transfer band of DENAB are adequately accommodated by a single line.

Introduction

Mechanisms. *cis*- and *trans*-azobenzene isomers occupy adjacent energy minima on a multidimensional potential energy surface. The barrier separating the two minima is formed by an avoided crossing of *cis* and *trans* surfaces. Since electronically excited states need not be considered, the mechanism of the cis-trans isomerization is known to the extent that it is merely a matter of activating one or more vibrational normal modes.

The transition state will be a region along the top of the barrier that minimizes the free energy of activation. It will be low in energy relative to other parts of the barrier, to minimize the enthalpy of activation, but also broad (i.e., rich in low energy paths) so as to maximize the entropy.

The vibrational modes most likely to be involved are torsion about the N=N bond, angle distortion of one or

both of the N-N-aryl bond angles, and torsion about the N-aryl bond. It should be noted that, since vibrational modes can interact, combined modes are entirely possible and may well offer a more favorable path than any one mode alone.

The choice of vibrational modes has been the subject of controversy. On one side it is claimed that all azobenzene isomerizations proceed by inversion, i.e., distortion of one of the N-N-aryl bond angles.³⁻⁵ This is sometimes called the rehybridization mechanism, since the angle-widening phase of the vibration changes the bond hybridization from sp²-sp² to one more like the sp-sp of a linear N-N-C conformation. Marcandalli et al.⁴ have shown that a plot of log *k* for a series of 4-substituted 4'-(diethylamino)azobenzenes in DMF vs. σ^+ and σ^- breaks sharply into two linear parts. The ρ values are -3.15 for the electron-releasing substituents and +10.2 for the electron-withdrawing substituents. Although this would

(1) For previous papers, see: (a) Sigman, M. E.; Lindley, S.; Leffler, J. E. *J. Am. Chem. Soc.* 1985, 107, 1471. (b) Sigman, M. E.; Leffler, J. E. *J. Phys. Chem.* 1986, 90, 6063. (c) Sigman, M. E.; Leffler, J. E. *J. Org. Chem.* 1987, 52, 1754.

(2) Sigman, M. E. "Investigation of Supercritical Carbon Dioxide as a Medium for Organic Reactions" Dissertation, Florida State University, 1986.

(3) Andersson, J. *J. Photochem.* 1983, 22, 245.

(4) Marcandalli, B.; Pellicciari-Di Liddo, L.; Di Fede, C.; Bellobono, I. R. *J. Chem. Soc., Perkin Trans. 2* 1984, 589.

(5) Nishimura, N.; Tanaka, T.; Asano, M.; Sueishi, Y. *J. Chem. Soc. Perkin Trans. 2* 1986, 1839.